

Electronic Supplementary Information

Immobilization of Nattokinase-loaded Red Blood Cells on the Surface of Superhydrophobic Polypropylene Targeting Fibrinolytic Performance

Chunming Li,^{a,b} Wei Ye,^a Jing Jin,^{*,a} Xiaodong Xu,^c Jingchuan Liu^a and Jinghua Yin^{*a}

^a *State Key Laboratory of Polymer Physics and Chemistry, Changchun Institute of Applied Chemistry, Chinese Academy of Sciences, Changchun 130022, PR China*

^b *University of Chinese Academy of Sciences, Beijing 100049, PR China*

^c *Polymer Materials Research Center, College of Materials Science and Chemical Engineering, Harbin Engineering University, Harbin 150001, PR China*

1. Materials and methods

1.1 Materials

Polypropylene (GM1600E) power was obtained from Shanghai Petrochemical Company. N-isopropylacrylamide (NIPAAm) and acrylic acid (AA) were obtained from J&K Chemical Ltd. Concanavalin A (Con A) was purchased from Sigma-Aldrich chemical Co. N-(3-dimethylaminopropyl)-N'-ethylcarbodiimide hydrochloride (EDC) and N-Hydroxysuccinimide (NHS) were purchased from Aladdin reagent company. Nattokinase (NK, 410 IU/g) was obtained from Wako (Japan). 1,1'-dioctadecyl-3,3,3',3'-tetramethylindocarbocyanine perchlorate(DiI) was purchased from Beyotime Institute of Biotechnology. Phosphate-buffered saline (PBS, 0.01 M phosphate buffer, pH 7.4) was prepared freshly. The other solvents and reagents were AR grade and used without further purification.

1.2 Preparation of superhydrophobic-polypropylene (PP)

A stable superhydrophobic-PP platform in atmosphere was fabricated using xylene as a good solvent and acetone as a non-solvent¹. In brief, 0.3 g of granulated PP was added to a flask containing 15 mL of xylene. PP solution was heated to approximately 120 °C when it was constantly stirred for 30 minutes by a magnetic stirring bar in atmosphere to form a precursor. Then, 6 mL acetone was added into the PP mixture at a rate of 2 mL·s⁻¹. After stirring the mixed solution for 2 minutes, a few drops of the mixture were then dipped onto a cleaned glass substrate. The superhydrophobic-PP platform was obtained after dried at 70 °C in a vacuum oven to remove the solvent.

1.3 Preparation of Con A-conjugated polymer brush on the superhydrophobic-PP surface.

1.3.1 Preparation of NIPAAm and AA modified responsive polymer brush.

O₂ plasma pretreatment and UV-irradiated techniques were combined to graft NIPAAm and AA on the surface of the superhydrophobic-PP. The superhydrophobic-PP was subjected to oxygen plasma (DT-03 plasma apparatus Suzhou Omega

Technology Co., Ltd.) at a pressure of approximately 15 Pa, 120 s. 20 μ L of monomer solution (prepurged with Ar) was deposited onto the superhydrophobic-PP surface. The obtained PP film was placed between two pieces of quartz plate and irradiated under UV light (high-pressure mercury lamp, 400 W, main wavelength = 380 nm) for 5 min. All the grafting PP films were washed with ethanol and water in succession to remove residual monomers. Finally, the modified superhydrophobic-PP films with different grafting ratios were obtained. As a control experiment, the same grafting polymerization was performed on the surface of the flat-PP.

1.3.2 Conjugation of Con A on the grafting surface

The modified PP film was activated in 0.4 M EDC and 0.1 M NHS for 1 h at 4 °C, and then washed twice with PBS and equilibrated in 0.1 M MES. 50 μ L 0.1 mg/mL Con A PBS solution was added onto the activated film for 12 h. Then the films were washed with PBS three times. After washed with PBS three times, the Con A-conjugated PP film was fabricated.

1.4 Surface characterization

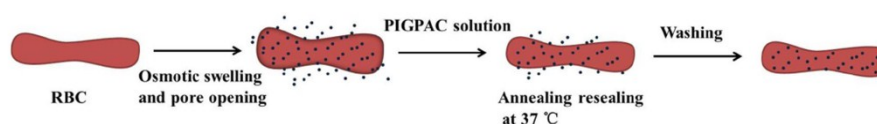
The surface chemical structure of the modified PP film was analyzed by Fourier transform infrared spectroscopy (FTIR, BRUKER Vertex 70) with an attenuated total reflection unit (ATR crystal, 45°) at a resolution of 4 cm^{-1} for 32 scans. The chemical composition of modified PP film was characterized by X-ray photoelectron spectroscopy (XPS, VG Scientific ESCA MK II Thermo Advantage V 3.20 analyzer) with Al/K ($h\nu = 1486.6$ eV) anode mono-X-ray source. All the films were completely vacuum-dried prior to use. The releasing angle of the photoelectron for each atom was fixed at 90°. Surface spectra were collected over a range of 0–1200 eV and high-resolution spectra of C 1s, N 1s, O 1s, and Cl 1s regions were collected. The atomic concentrations of the elements were calculated by their corresponding peak areas.

Static water contact angles of PP films were measured on a drop shape analysis instrument (DSA 100, Kruss GmbH, Hamburg, Germany) by placing 2 μ L of distilled

water at two different temperatures (37 °C and 25 °C). Six parallel experiments were made on a single sample to obtain the average value of contact angle.

1.5 Loading red blood cells (RBCs) with NK

Fresh blood collected from a healthy rabbit was mixed immediately with a 3.8 wt.% solution of sodium citrate at a dilution ration of 9:1. The RBCs were washed three times with PBS. The detailed NK-loaded RBCs procedure is shown in Scheme S1. 300 μ L of RBC pellets and 300 μ L of solution of NK (10 mg/mL) in water were mixed, resulting in hypotonic conditions^{2, 3}. The RBCs were incubated under slightly stirring for 1 h at 4°C , resealed (through reconstitution of isotonicity) by adding 30 μ L of PIGPAC solution (5mM adenine, 100mM sodium phosphate, 100mM sodium pyruvate, 100mM inosine, 100mM glucose, and 12% sodium chloride, pH 7.4), and then incubated at 37 °C for 1 h. The NK-loaded RBCs were washed three times with PBS to remove free hemoglobin and excess NK. The surface morphology of RBCs was observed with a field emitted scanning electron microscopy (FESEM, XL 30 ESEM FEG, FEI Company).



Scheme S1. Schematic representation of RBC loading procedure

1.6 Whole blood cell attachment

Fresh blood collected from a healthy rabbit was mixed immediately with a 3.8 wt.% solution of sodium citrate at a dilution ration of 9:1. Flat- and superhydrophobic-PP films (1 cm \times 1 cm) were incubated for 2 h in PBS and placed in a tissue culture plate. 2 mL of fresh whole blood solution was placed on the substrate surface in each well of the tissue culture plate for 60 min at 37°C . After the films were washed with PBS, blood cells adhered to the film were fixed by 2.5 wt. % glutaraldehyde at 4°C for 10 h. Finally,

the films were washed with PBS three times and dehydrated with a series of ethanol/water mixtures (30, 50, 70, 90, and 100 vol. % ethanol; 30 min in each mixture). The obtained films were gold sputtered in vacuum and observed with field emission scanning electron microscopy (SEM, FESEM, XL 30 ESEM FEG, FEI Company).

1.7 Cell capturing and releasing experiment

The Con A-conjugated PP films were placed into 12-well culture plate and 1 mL red blood cells stained with DiI were added. After incubated for 30 min at 37 °C, the films were gently washed 3 times with PBS solution. Finally, the cells were imaged by confocal laser scanning microscopy (CLSM, CARL ZEISS LSM 700, Germany). After RBCs-capturing, the films were transferred into a 4°C refrigerator or 25°C incubator for 30 min, and then gently rinsed with PBS 3 times, finally imaged by CLSM (CARL ZEISS LSM 700, Germany).

1.8 Fibrinolysis activity of films that captured NK loaded red blood cells

Fibrinolytic activity of the modified superhydrophobic-PP that captured NK-loaded RBCs was determined by a fibrin plate method^{4,5}. Briefly, 4 mL of fibrinogen solution (10 mg/mL in PBS) was poured into a culture dish (\varnothing =5 cm). Then 30 μ L of thrombin (60 IU/mL) was added to the solution and mixed well by rotating the plate. The plate was incubated for 3 h at room temperature to prepare a fibrin plate. To assess the activity of the PP that captured RBCs (0.5 cm in diameter), the modified PP was spotted on a fibrin plate, and the area of dissolved fibrin around the spotted PP films after 12 h was measured at 25°C.

1.9 Statistics

The analysis involved both counting of the RBCs (per surface area) and the analysis of the radius of thrombolysis effect using the software Image-Pro Plus. The data from multiple separate experiments were analyzed and reported as the mean \pm standard error (SE) of the mean. The data were analyzed by the one-way ANOVA method; the

statistical significance was accepted when $p < 0.05$. Each result is an average of at least three parallel experiments.

2. Water contact angle of the superhydrophobic-PP

Figure S1 shows the water contact angle of the superhydrophobic-PP. The water contact angle of the fabricated PP is sharply increased to 156° , indicating the formation of superhydrophobic structure. The effects of different conditions and parameters such as concentration, temperature, and the amount of acetone on the morphology, the contact and sliding angles have been investigated in details¹. The modified superhydrophobic-PP surface presents hierarchical structures similar to those of lotus leaves. The optimal condition investigated by Ji¹ was chosen. Acetone acts as a polymer precipitator by increasing the extent of polymer phase separation between the two phases of polymer plus small amount of xylene and acetone plus xylene. Crystallization time decreased and smaller aggregates were formed. This process led to separation into two macroscopic phases: one polymer-rich and the other polymer-poor⁶. Crystallization started in the polymer-rich phase by the formation of crystal nuclei and the solvent then evaporated from these pores.

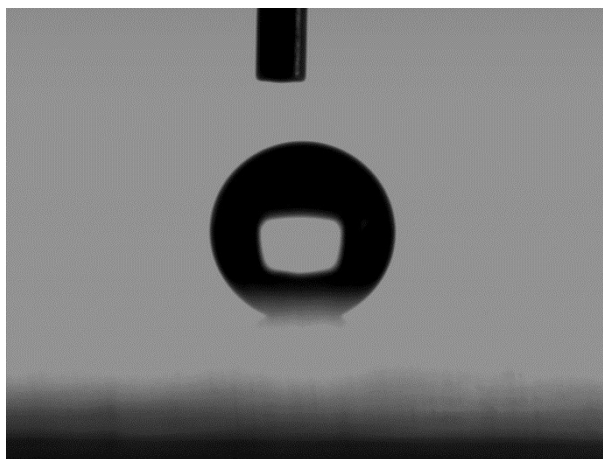


Figure S1. Water contact angle of PP that was fabricated using xylene as a good solvent and acetone as a non-solvent.

3. Surface structure characterization

The ATR-FTIR of the neat and modified PP is shown in Figure S2. Compared with the neat PP, there are two new peaks at 1543 and 1647 cm^{-1} for PP-g-P(NIPAAm), which are corresponding to the O=C-N-H stretch vibrations. After co-grafting with AA, a new peak at 1716 cm^{-1} is assigned to carboxyl group in AA. These results indicate that the polymer brushes are grafted on the PP surface successfully.

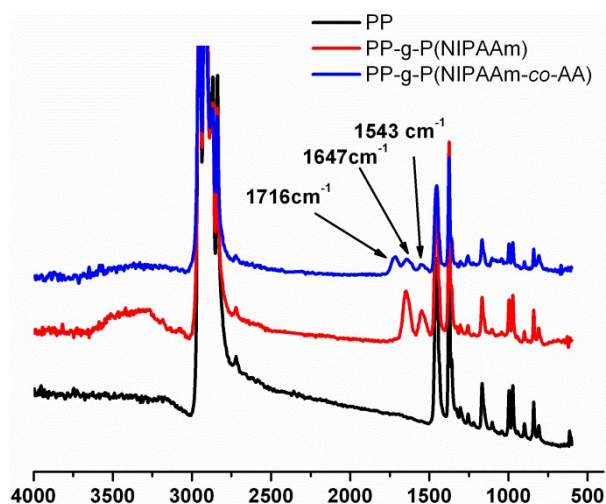


Figure S2. ATR-FTIR spectra of PP, PP-g-P (NIPAAm) and PP-g-P (NIPAAm-co-AA).

The surface structure compositions of modified PP were also confirmed by XPS. After grafting of NIPAAm and AA, the appearance of O1s and N1s binding energy at 532 eV and 399.5 eV in the wide scan spectra confirm the presence of NIPAAm and AA on the surface of modified PP (Figure S3b). The N1s peak at the binding energy of 399.5 eV is assigned to amide nitrogen (-N-C=O), which also confirm the presence of PNIPAAm on the surface. The appearance of S2p at 168 eV and increment of N1s on the surface of the Con A-conjugated PP (Figure S3c and 3f) indicate that the Con A is conjugated onto the modified PP surface successfully. Figure S4 shows the C 1s core-level spectra. The spectra of grafting PP (Figure 4b) can be curve-fitted into four-peak components. The four-peak components with binding energies at about 284.6, 285.5, 287.6 and 288.5 eV are attributed to the C-H, C-O(C-N), N-C=O, and -COOH species, respectively⁷. After Con A conjugation, the constituent of N-C=O increases and -

COOH decreases, which is because of the reaction between carboxyl group in polymer brushes and amino group in protein.

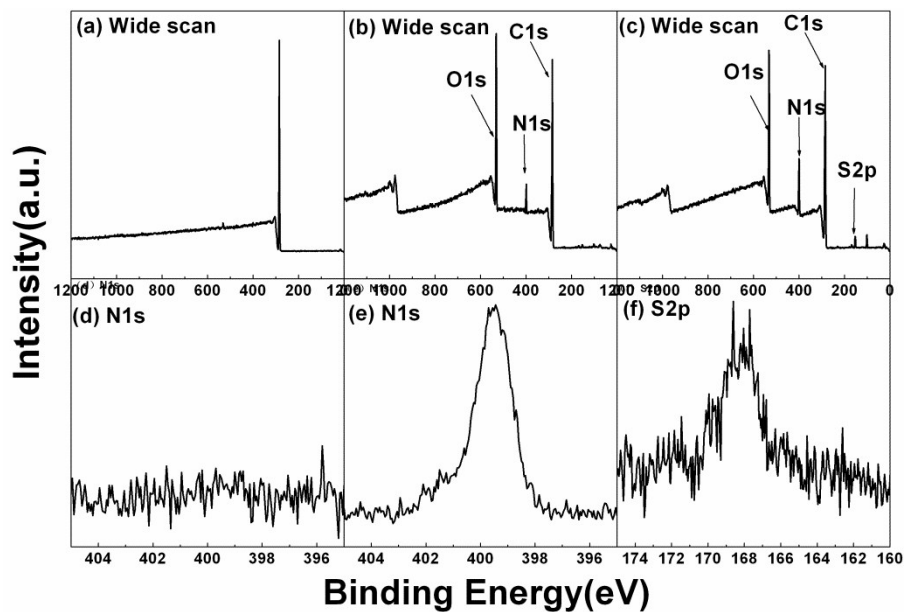


Figure S3. Wide scan spectra of (a) PP, (b) PP-g-P(NIPAAm-*co*-AA) and (c) PP-g-P(NIPAAm-*co*-AA)-Con A, (d) N1s core-level spectra of PP, (e) N1s core-level spectra of PP-g-P(NIPAAm-*co*-AA), and (f) S2p core-level spectra of PP-g-P(NIPAAm-*co*-AA)-Con A.

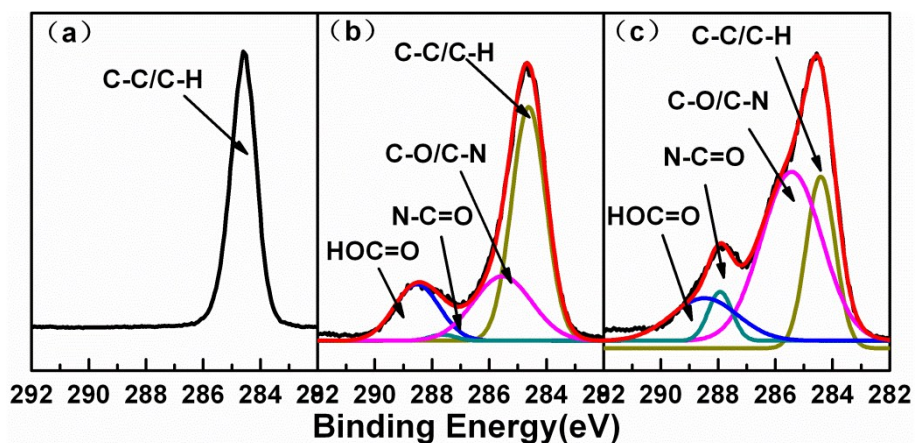


Figure S4. C1s core-level spectra of (a) PP, (b) PP-g-P(NIPAAm-*co*-AA), and (c) PP-g-P(NIPAAm-*co*-AA)-Con A.

4. Con A conjugated onto the modified PP surface with different NIPAAm: AA ratios

The modified superhydrophobic-PP surface has switchable adhesion property that is responsive to both temperature and pH by simply grafting with poly(NIPAAm-co-AA) copolymer⁷. Figure S5 shows the fluorescence intensity of FITC-Con A conjugated onto the PP-g-P (NIPAAm-co-AA) surface with different monomer ratios. It can be used to investigate the influence of the monomer mole ratio ($M_{\text{NIPAAm}}: M_{\text{AA}}$) on the conjugation of Con A. The amount of FITC-Con A on PP surface increases with increasing of mole ratio of $M_{\text{AA}}: M_{\text{NIPAAm}}$, which is attributed to more carboxyl groups on the grafting polymer brushes surface. The amount of Con A conjugated onto the modified PP surface could be regulated by the monomer mole ratio.

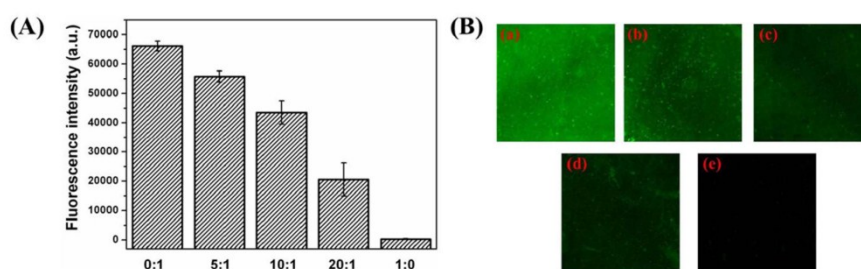


Figure S5. (A) Fluorescence intensity of FITC-Con A immobilized onto PP-g-P (NIPAAm-co-AA) at different monomer ratio of $M_{\text{NIPAAm}}: M_{\text{AA}}$. (B) Fluorescence images of FITC-Con A immobilized onto PP-g-P(NIPAAm-co-AA) at different monomer ratios of NIPAAm :AA (a) 0:1 (b) 5:1 (c) 10:1 (d) 20:1 (e) 1:0.

5. RBCs release at 25°C

The temperature of blood and component during storage, filtration, or processing is an important factor in hemolysis⁸. The deformability of RBCs is greatly influenced by temperature and the optimum temperature of RBCs during storing and processing is 4°C. Released RBCs on modified PP at 4°C is shown in Figure 2. Besides, the release studies were also conducted at 25°C (Figure S6). The capture and release performance

was similar to 4°C. A great number of RBCs were captured on the modified superhydrophobic-PP at 37°C(Figure S6a) and released at 25°C(Figure S6b). The quantitative result of the RBCs that were captured and released on the surface was shown in Figure S6c. The number of captured RBCs was 3.77×10^5 cells per surface area, while the number was decreased to 0.52×10^5 cells per surface area after released at 25°C. Combined with the results in Figure S6 and Figure 2, we concluded that RBCs could be also released efficiently at the temperature under LCST of PNIPAAm such as 25°C and 4°C.

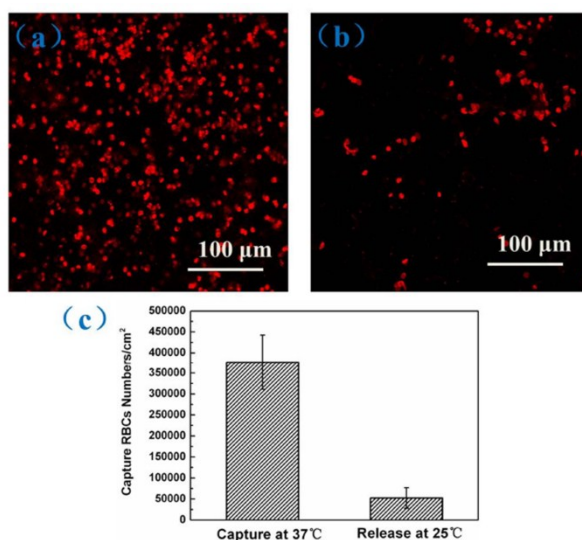


Figure S6. RBCs were captured on modified superhydrophobic-PP at 37°C(a) and release at 25°C(b) and quantitative evaluations of cell capture/release performance per surface area (c).

6. RBC loaded with FITC-NK

RBCs represent a potential natural drug carrier system due to the ability of their membranes to be opened and resealed^{2, 9}. A lot of drugs have been loaded by RBCs such as immunosuppressive drugs¹⁰, L-Asparaginase¹¹, vaccine³, amikacin¹², and pravastatin¹³. There are two major approaches to the association between pharmaceuticals and erythrocyte carriers¹⁴. The most widely used approach is drug encapsulation in erythrocytes using encapsulation methods. The second approach is reversible or irreversible attachment of the ligand to RBC membrane. The

encapsulation methods include osmosis-based methods, electroporation, and drug-induced endocytosis. Here, we choose hypotonic dilution to load NK into RBCs.

Figure S6 displays the CLSM and SEM images of FITC-NK-loaded RBCs and unloaded RBCs (treated with water). The intense fluorescence (Figure S7a) is observed on FITC-NK loaded RBCs sample, which infers that NK is loaded into RBCs successfully. The morphology of RBCs is observed by SEM (Figure S6c and S6d). Most of the NK-loaded RBCs keep the normal shape, whereas the unloaded RBCs display different stages of biconcave. Cup-form, stomatocyte, spherocyte (spherical erythrocytes), echinocyte and irregular shapes are evident in the sample of unloaded RBCs (Figure S7d)³. The extent of irreversible shape changes occurs in loaded RBCs compared to normal cells, is a function of the loading method used which, in turn, exert different changes in RBCs shape and surface properties³. The SEM results indicate that NK-loaded RBCs keep normal shape because NK in water maintains part osmotic pressure. The shape change is reversible while that of the RBCs treated with water is irreversible. The above results show that NK is loaded into RBCs and the RBCs keep the normal shapes.

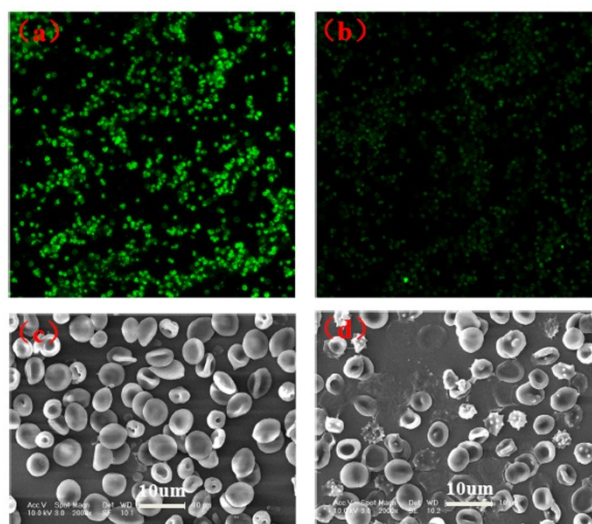


Figure S7. Fluorescence and SEM images of (a and c) FITC-NK loaded RBC and (b and d) Blank RBC

References:

1. Ji, H. Y.; Chen, G.; Hu, J.; Yang, X. F.; Min, C. Y.; Zhao, Y. T. *J. Disper. Sci. Technol* 2013, **34**, 134-139.

2. Delcea, M.; Sternberg, N.; Yashchenok, A. M.; Georgieva, R.; Bäumlner, H.; Möhwald, H.; Skirtach, A. G. *ACS Nano* 2012, **6**, 4169-4180.
3. Hamidi, M.; Zarei, N.; Zarrin, A. H.; Mohammadi-Samani, S. *International Journal of Pharmaceutics* 2007, **338**, 70-78.
4. Edward, N. *Journal of Clinical Pathology* 1972, **25**, 335-337.
5. Teramura, Y.; Iwata, H. *Bioconjugate. Chem.* 2008, **19**, 1389-1395.
6. Erbil, H. Y.; Demirel, A. L.; Avci, Y.; Mert, O. *Science* 2003, **299**, 1377-80.
7. Cheng, Z.; Lai, H.; Du, M.; Zhu, S.; Zhang, N.; Sun, K. *Soft Matter* 2012, **8**, 9635-9641.
8. S. O. Sowemimo-Coker, *Transfus. Med. Rev.*, 2002, **16**, 46-60.
9. Biagiotti, S.; Paoletti, M. F.; Fraternali, A.; Rossi, L.; Magnani, M. *Iubmb Life* 2011, **63**, 621-631.
10. Biagiotti, S.; Rossi, L.; Bianchi, M.; Giacomini, E.; Pierigè, F.; Serafini, G.; Conaldi, P. G.; Magnani, M. *Journal of Controlled Release* 2011, **154**, 306-313.
11. Kwon, Y. M.; Chung, H. S.; Moon, C.; Yockman, J.; Park, Y. J.; Gitlin, S. D.; David, A. E.; Yang, V. C. *Journal of Controlled Release* 2009, **139**, 182-189.
12. Gutiérrez Millán, C.; Bax, B. E.; Castañeda, A. Z.; Marinero, M. L. S.; Lanao, J. M. *Translational Research* 2008, **152**, 59-66.
13. Harisa, G. I.; Ibrahim, M. F.; Alanazi, F. K. *Arch Pharm Res* 2012, **35**, 1431-9.
14. Hamidi, M.; Zarrin, A.; Foroozesh, M.; Mohammadi-Samani, S. *J. Control Release.* 2007, **118**, 145-160.